2017

The Intrinsic Variability of the Water Vapor Saturation Ratio Due to Mixing

Jesse Anderson
Michigan Technological University, jcanders@mtu.edu

THE INTRINSIC VARIABILITY IN THE WATER VAPOR SATURATION RATIO DUE TO TURBULENCE

By

Jesse Charles Anderson

A THESIS

Submitted in partial fulfillment of the requirements for the degree of

MASTER OF SCIENCE

In Applied Physics

MICHIGAN TECHNOLOGICAL UNIVERSITY

2017

This thesis has been approved in partial fulfillment of the requirements for the Degree of MASTER OF SCIENCE in Applied Physics.

Department of Physics

Thesis Advisor: *Dr. Will Cantrell*

Committee Member: *Dr. Raymond Shaw*

Committee Member: *Dr. Mark Kulie*

Department Chair: *Dr. Ravindra Pandey*

Contents

Acknowledgments

Michigan Technological University, Department of Physics, Atmospheric Sciences

National Science Foundation

Abstract

The water vapor concentration plays an important role for many atmospheric processes. The mean concentration is key to understand water vapor's effect on the climate as a greenhouse gas. The fluctuations about the mean are important to understand heat fluxes between Earth's surface and the boundary layer. These fluctuations are linked to turbulence that is present in the boundary layer. Turbulent conditions are simulated in Michigan Techs multiphase, turbulent reaction chamber, the Π chamber. Measurements for temperature and water vapor concentration were recorded under forced Rayleigh- Bénard convection at several turbulent intensities. These were used to calculate the saturation ratio, often referred to as the relative humidity. The fluctuations in the water vapor concentration were found to be the more important than the temperature for the variability of the saturation ratio. The fluctuations in the saturation ratio result in some cloud droplets experiencing a higher supersaturation than other cloud droplets, causing those "lucky" droplets to grow at a faster rate than other droplets. This difference in growth rates could contribute to a broadening of the size distribution of cloud droplets, resulting in the enhancement of collision-coalescence. These fluctuations become more pronounced with more intense turbulence.

1. Introduction

In the atmosphere, the concentration of water vapor is important in that it has several roles in our climate system. The mean water vapor concentration plays is role as a greenhouse gas and the fluctuations about its mean are key to understand the propagation of electromagnetic radiation and boundary layer heat fluxes. Both the mean and the variation around the mean are important for growth of cloud droplets [1, 2, 3, 4].

The most common way to describe the amount of water vapor in the atmosphere is the relative humidity or the saturation ratio, shown in Equation 1.1. This is done because it neglects the total amounts of ice and liquid water that coexists in the atmosphere.

$$S_{liquid} \equiv \frac{n}{n_s} = \frac{e}{e_s(T)} \tag{1.1}$$

where n is the molar density of water vapor in air and e is the partial pressure of water vapor in air. n_s and e_s corresponds to the molar density and partial pressure of water vapor, respectively, at equilibrium with a plane surface of pure liquid water at a given temperature T. e_s has a temperature dependence as noted in the final

term of Equation 1.1. The value of S is viewed in relation to equilibrium where S=1. Values of S above 1 thermodynamically forces condensation, where values below 1 forces evaporation [5, pg. 174].

The magnitude of S important for the growth of a cloud droplets by the condensation of vapor. That growth is often written similar to Equation 1.2;

$$\frac{dm}{dt} = 4\pi r \rho_l G \left(S - S_K\right) \tag{1.2}$$

where m and r are the mass and radius of the droplet, respectively. ρ_l is the density of liquid water. S_K is the saturation ratio at the surface of the droplet, and G incorporates surface and heat transfer effects. The difference between the saturation ratio at the surface and the saturation ratio far away from the droplet is the driving factor for the growth of the droplet [5, pg. 324]; where the condensation (or evaporation) is caused by water vapor following the concentration gradient. Although this can be written as a difference in the water vapor concentrations, we have followed the development of writing this difference as a difference between the the saturation ratios.

For a single cloud droplet, the calculations for growth rate shown in Equation 1.2 are not difficult. When applied to an ensemble of cloud droplets this becomes significantly

more complex; which has been noted by several authors [1, 2, 3, 4]. It is tempting to assume the value of S is uniform throughout the air parcel, where the mean saturation ratio is felt by each cloud droplet. In truth, the value of S is more ambiguous than simply the mean value. S is not uniform due to several different factors; the chance clustering of droplets and random fluctuations about the mean caused by turbulence. Clusters of cloud droplets compete for water vapor with their neighbors and lower the local water vapor concentration as a result of condensation [1, 3]. As droplets grow by condensation, a release of latent heat increases the local temperature, [4]. From Equation 1.1 this increase in temperature lowers the value of S. Turbulence induces random fluctuations in the scalar fields of temperature and water vapor concentration [2], which clearly causes fluctuations in S.

Having established that S is not uniform for each individual cloud droplet, our goal is to quantify the variability of S in a turbulent environment; keeping in mind that S can vary from fluctuations in the water vapor concentration and temperature. Using Michigan Tech's cloud chamber, we have measured the water vapor concentration and temperature over long periods of time. Measurements were taken at several different turbulent intensities with and without cloud formation. With this data set

we aim to quantify the variability in S, which will contribute to the understanding of atmospheric processes, such as the growth of an ensemble of cloud droplets.

2. Methods

The initial conditions for cloud formation were created in the Π Chamber with the cylindrical insert in place. The chamber is described in more detail in Chang et al. [6], and only the necessary details will be described here. The cylinder restricts the Π Chamber to a volume of 3.14m^3 and gives the chamber its name. Mixing was caused by forced Rayleigh-Bénard convection, where $T_{bottom\,plate} > T_{top\,plate}$. Temperature differences (ΔT) for 4, 6, 8, and 9 K between the top and bottom plates are used for these measurements. The mean temperature for each ΔT is 10^oC.

Temperature was measured at eight different locations in the chamber, using resistance temperature detectors (RTD, Minco), shown in 2.1, and were recorded at 1 Hz using a Lakeshore Temperature Monitor (model 331). Water vapor concentration was recorded at 20 Hz using a LI-COR LI-7500A Open Path CO_2/H_2O Gas Analyzer. The LI-COR has a measuring path length of $\approx$ 12.5cm. For the purposes of any calculation of S, the closest RTD to the LI-COR (T7) has been used in conjunction with the LI-COR. T7 is located $\approx$ 6cm above the LI-COR.

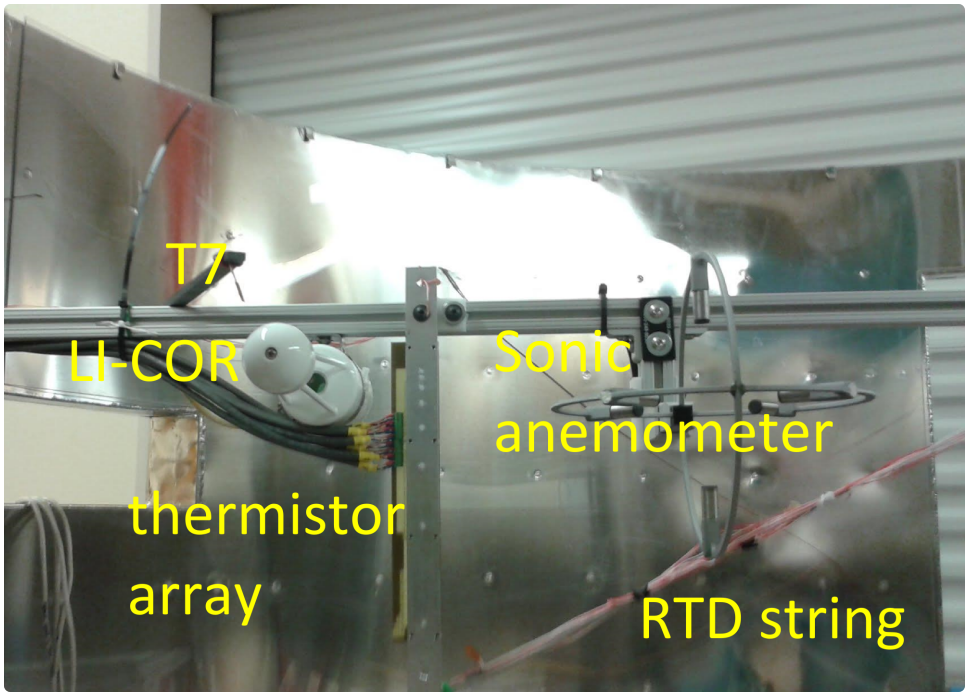

Figure 2.1: Photograph showing the relative positions of the equipment in the cylinder. The LI-COR and sonic anemometer are mounted halfway between the plates. Note that RTD 7 (T7) is placed just above the LI-COR. Another RTD is just above the thermistor array. The remaining six are strung on a line running diagonally across the cylinder. The LI-COR is 46cm away from the cylinder wall. The thermistor array was mounted vertically 6.5 cm away from the LI-COR and the Sonic was mounted 27 cm away from the LICOR.

3. Results

3.1 Moist convection

Initially, a wet turbulent environment was created in the absence of a cloud to remove any influence aerosols have on the fluctuations of n, T and S. These conditions will be referred to as moist convection. During moist convection a typical time series is shown in Figure 3.1. The mean value for each measurement is relatively steady over the course of several hours. This indicates that steady state conditions can be created and held for long periods of time with a $\overline{T} \approx 10.5\ C$. Fluctuations about that mean value are clearly present across a range of timescales; from less than a second, to minutes. Fluctuations associated with the mean flow of convection can be seen, with a period around one minute (these fluctuations are the subject of a paper in preparation (Niedermeir et al.) and will not be discussed here.). Small changes in the PID controls of the chamber can be seen in the time series of both measurements. These fluctuations have a period of 20 minutes to an hour.

Inspection of these fluctuations shows that there is a relative dispersion (standard deviation relative to the mean) of 1 to 2% for the water vapor concentration. The temperature on the other hand, has a relative dispersion orders of magnitude lower.

(Noting that the mean value for temperature is calculated in Kelvin, not Celsius.) This difference in the relative dispersion of water vapor concentration and temperature implies fluctuations in the water vapor concentration are the driving factor for any fluctuations in S, not the temperature.

The variation of the water vapor concentration, down sampled to 1Hz, is compared to the temperature difference between the top and bottom plates of the Π chamber. As previously noted, the PID system of the chamber induce a fluctuations with a period of around 20 minutes to an hour. These fluctuations were removed by taking the raw data smoothed with a 10 minute lowess filter and subtracting that curve from the raw data. The temperature measured by T7 is used to calculate the saturated water vapor concentration from the Clausius-Clapeyron equation, in order for the comparison between data sets to be made using the same units. From the trend in Figure 3.2, the intensity of turbulence clearly has an impact on the magnitude of the variance for the measurements of n and T. Again, the variation in the water vapor concentration is significantly larger than the variation of the temperature measurement. Over the range of measurements presented, the variance is linear with respect to the temperature difference.

The probability density function shown in figure 3.3 shows the residual fluctuations for the n and T at different ΔTs. The water vapor measurements were converted to 1 Hz. It is no surprise after inspecting Figure 3.2 that the width of each distribution

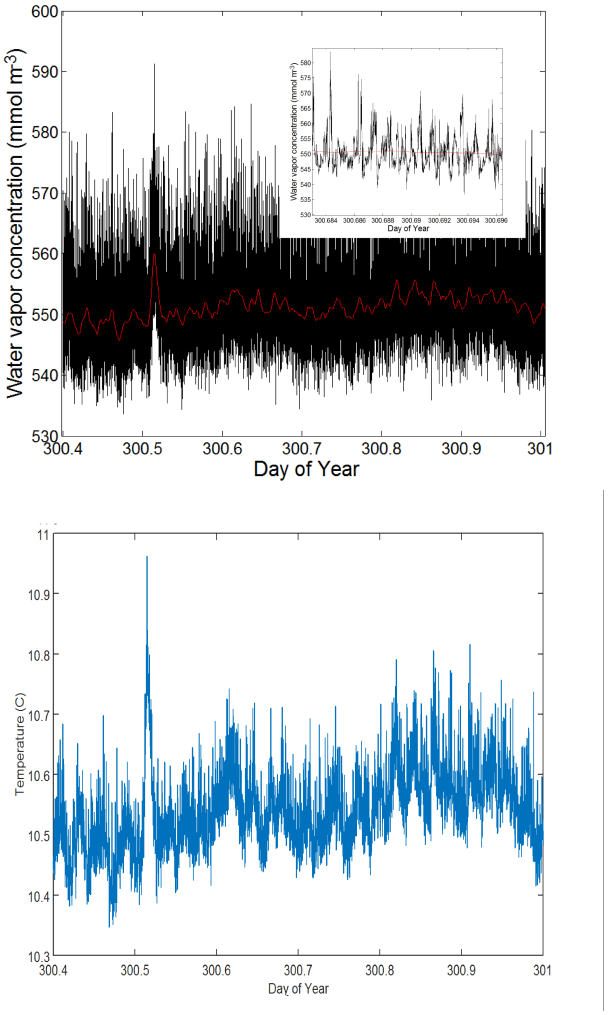

Figure 3.1: Typical time series of water vapor concentration and temperature during turbulent convection in the chamber. **Top panel:**Water vapor concentrations measured at 20 Hz for a temperature difference in the chamber of 6 K. The red line is a 10 minute running average. The inset to the panel is a subset, showing fluctuations at a finer temporal resolution. **Bottom panel:**Temperature measured with an RTD at 1 Hz (blue line) in the chamber for the same time period as the data shown in the top panel. Fluctuations about the mean on the time scales discussed above are evident here as well.

is impacted by the intensity of turbulence. A larger ΔT between the plates causes more prominent fluctuations around the mean. For both n and T, the distributions

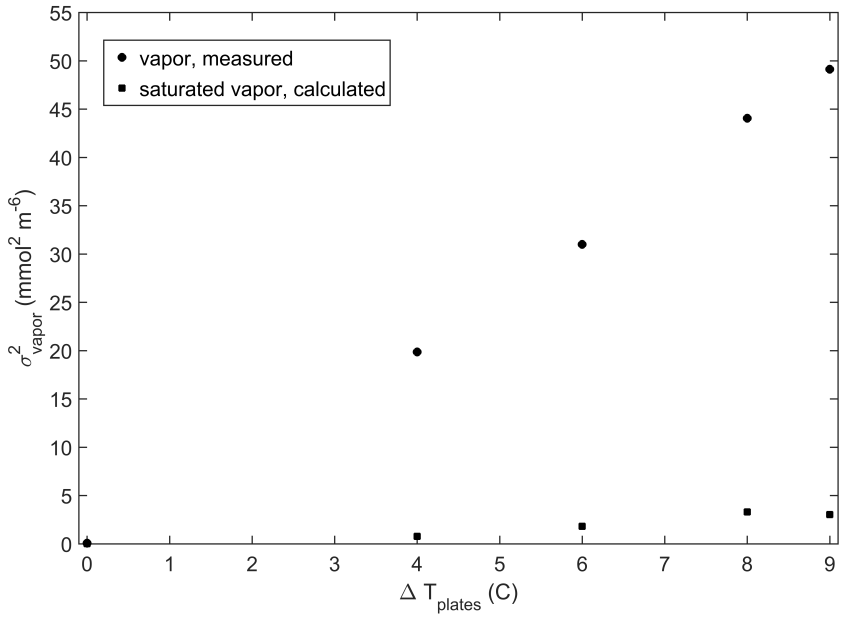

Figure 3.2: Variance in the water vapor concentration as a function of the temperature difference between the top and bottom plates in the chamber. To compare variances in measured water vapor concentrations and temperature, the measured temperature (T7) was used to calculate the saturation vapor density (see text).

are positively skewed; with large, infrequent deviations above the mean being more likely than deviations below. It is likely that this skewness is a consequence of the periodic mean circulation in the chamber. When a high pass filter is applied to the data set, the distribution is no longer skewed.

The scatter plot for $\Delta T = 6$ K of the water vapor concentration and temperature is shown in Figure 3.4. The water vapor concentration is down sampled to 1 Hz. The data is shown in relation to the Clausius-Clapeyron equation (S=1) and the mixing line. The mixing line is described in detail in Bohren and Albrecht (1998) [7, Sec. 3.8 and 6.7] and is calculated as a weighted mean of the air in contact with the top

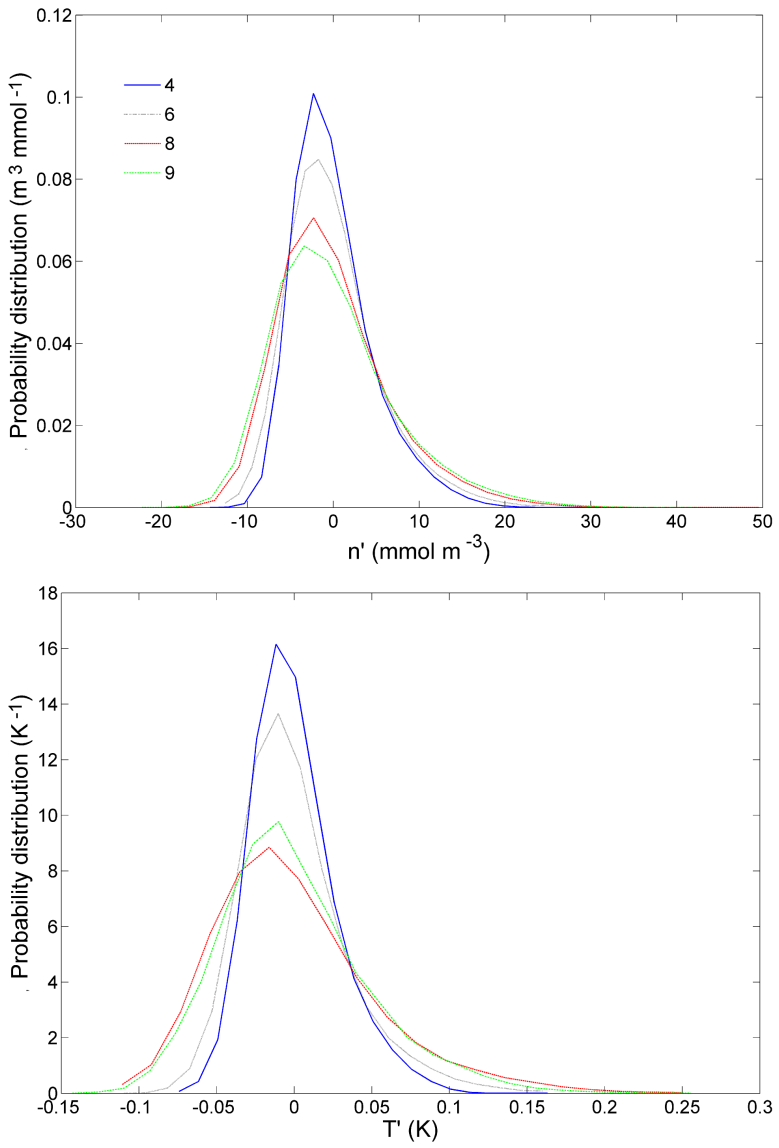

Figure 3.3: Probability distribution of fluctuations of water vapor concentrations (upper panel) and temperature (lower panel) about their respective means for temperature differences of 4, 6, 8, and 9 K between top and bottom plates in the chamber.

and bottom boundaries. Fluctuations off of the mixing line are are present for each temperature recorded by T7. Clearly the variability that is shown is greater than the variability that would be seen if the water vapor and temperature followed the mixing

line. These fluctuations are not likely to be an artifact of noise in the measurements, as evidenced by the variance in isothermal conditions shown in Figure 3.2, with a $\sigma_n^2 = 0.067$ (mmol^2 m^{-6}). A majority of the measurements of n at the measured temperature are above the Clausius-Clapeyron equation; supporting that conditions for cloud formation are met with the chamber being in a state of supersaturation. The mean water vapor concentration ($\overline{n}$) at each temperature tends to follow the trend of the mixing line; implying that fluctuations seen in the water vapor and temperature are not due to unknown amounts of air entering the Π chamber. The offset in $\overline{n}$ from the mixing line is most likely due to a combination of the absolute accuracy in the LI-COR and the fact that T7 is slightly displaced from the LI-COR. The contour lines corresponds to the joint probability distribution of n and T. The lines closer to the center correspond to a higher number of measurements for that temperature and water vapor concentration.

Returning to our goal of examining the fluctuations in the saturation ratio, Figure 3.5 shows S down sampled to 1 Hz, at the measured temperature. Again, a mean supersaturation is seen with a large majority of measurements of S above unity. Further more, the mean S at a given temperature is most often greater than unity. Significant fluctuations about the mean value of ≈ 1.02 are clearly present. These fluctuations range from ≈ 0.98 to ≈ 1.08.

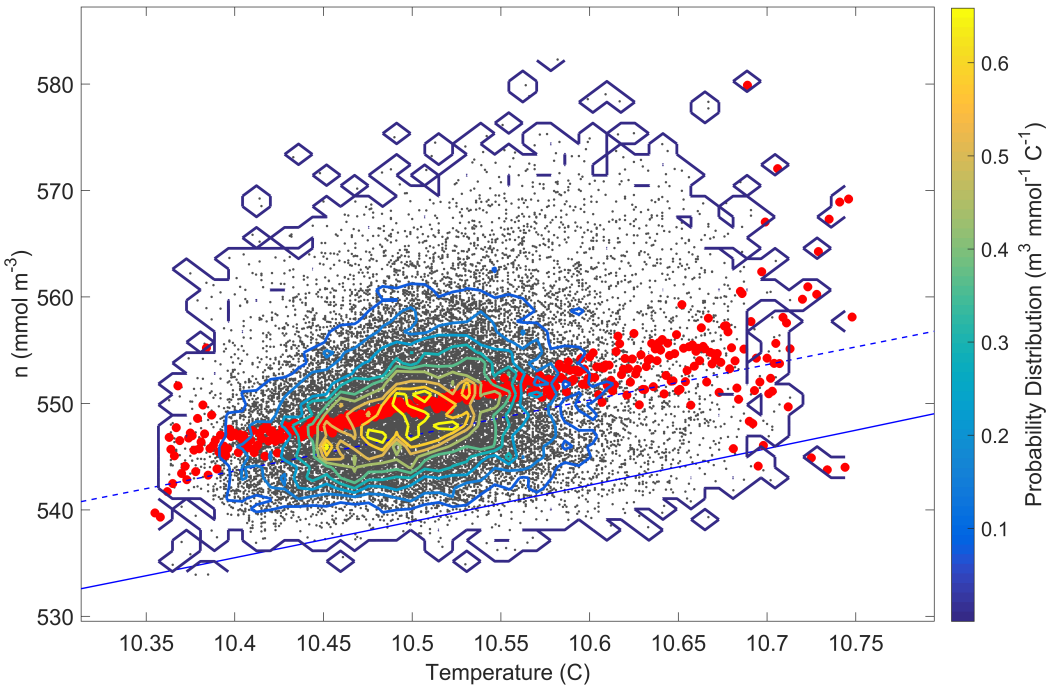

Figure 3.4: Water vapor concentrations in the chamber as a function of temperature for $\Delta T = 6$ K. The points are averages of the measured water vapor concentrations. The red circles are the mean water vapor concentration for a particular temperature. The solid blue line is the saturated water vapor concentration. The dashed blue line is the mixing line. The contour lines correspond to the joint probability distribution, shown on the color bar. The offset of $\overline{n}$ from the mixing line is most likely a combination of an offset in the absolute accuracy of the LICOR and the fact that the water vapor and temperature measurements are slightly displaced.

3.2 Comments on Measurements

In the calculation for S, the displacement of T7 and the LI-COR should be discussed. This displacement of T7 shown previously in Figure 2.1, where T7 is located $\approx$ 6cm away from the LI-COR. In addition the LI-COR has an optical path of $\approx$ 12.5cm; effectively smoothing fluctuations on a scale smaller than that volume. Comparatively,

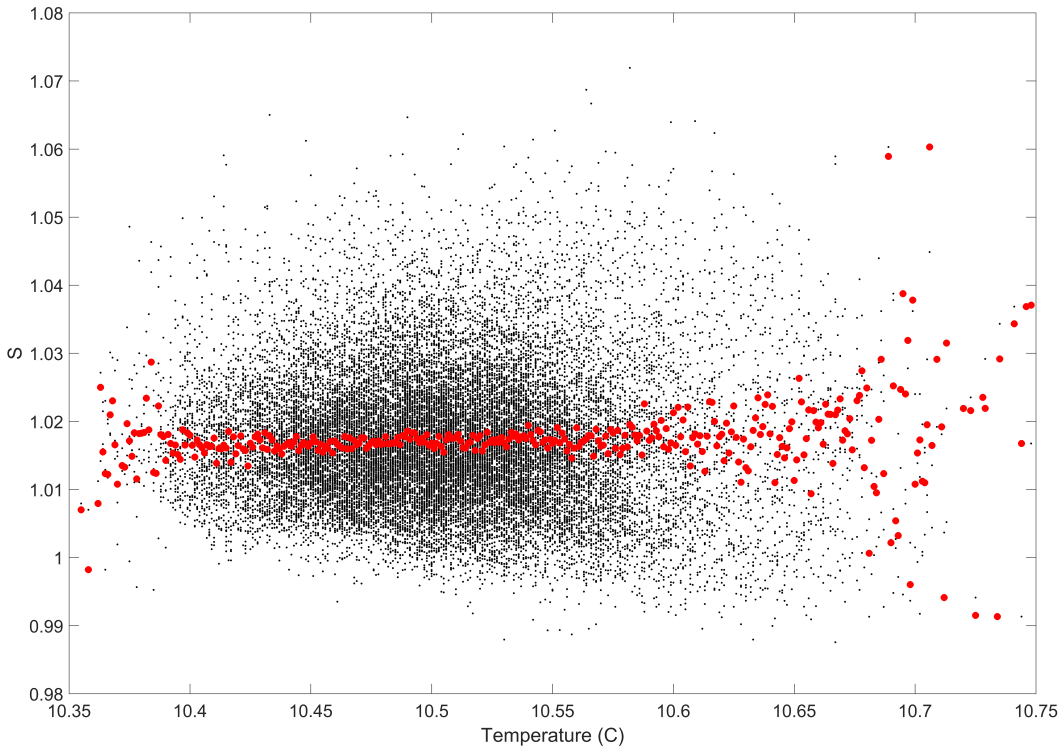

Figure 3.5: Saturation ratio as a function of temperature. S is calculated from the measured water vapor concentrations and the saturation vapor density. As in Figure 3.4, the black points are all values of S while the red circles are $\overline{S}$.

the RTDs are closer to point measurements. To address whether the displacement of T7 or the difference in the spatial scale of the sensors has an impact on the fluctuations of S, a new data set was measured under the same conditions as moist convection, with a $\Delta T = 6$K. This setup differs from the previous due to the placement of the RTDs; here three RTDs (T6, T7 and T8) are placed along the optical path of the LI-COR and T3 located 8cm away from the LI-COR. This setup shown in Figure 3.6.

With the setup shown in Figure 3.6, the temperature of the three RTDs spaced along the LI-COR's optical path (T6, T7, T8) are averaged at each time step, denoted

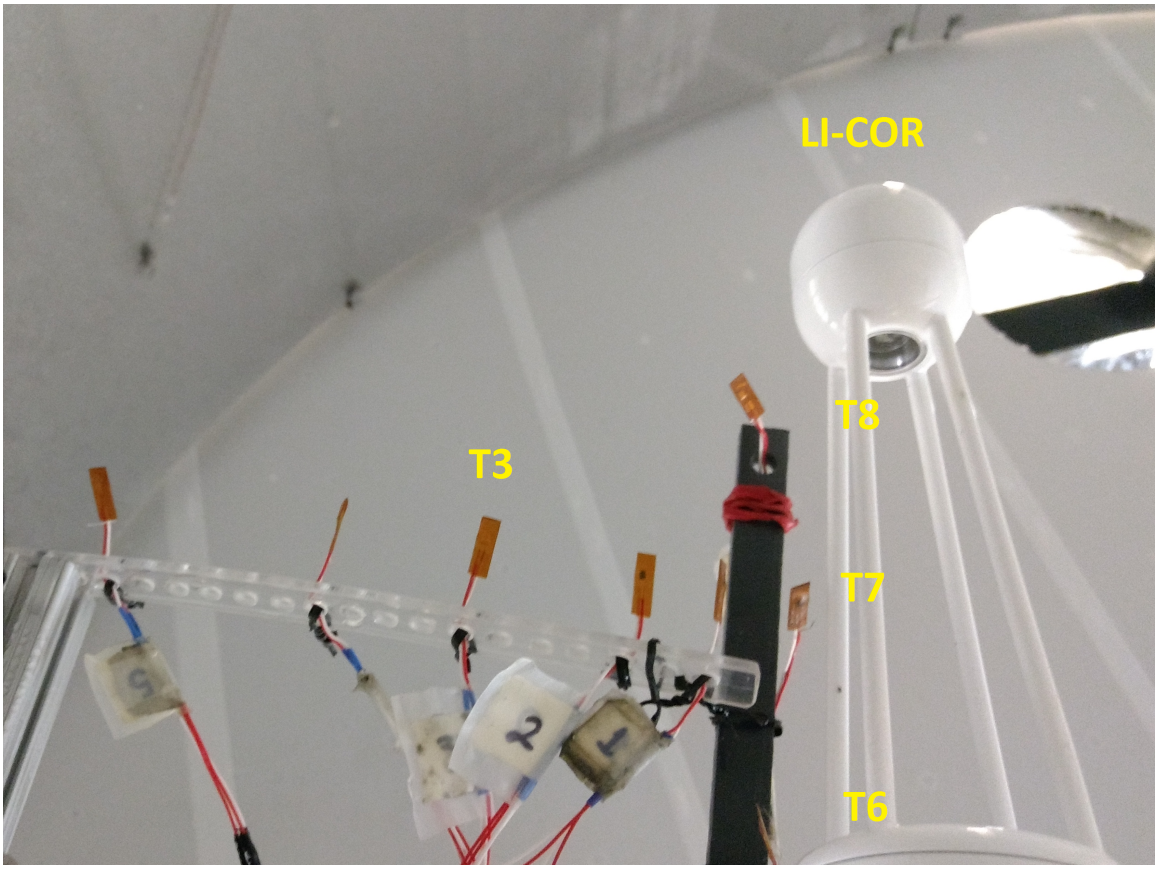

Figure 3.6: Photograph from below showing the equipment locations for the setup to test the impact of the temperature measurement being displaced from the LI-COR. T6 and T8 are placed on opposite ends of the LI-COR's optical path with T7 being located at the midpoint. T3 is placed 8cm away from T7.

as $< T6, T7, T8 >$ (note that this is not the overall mean of T6, T7 and T8). $< T6, T7, T8 >$ and T3 are used with the water vapor concentration converted to 1 Hz in order to calculate the saturation ratio, $S_{<T6,T7,T8>}$ and S_{T3} respectively. The resulting time series for $S_{<T6,T7,T8>}$ and S_{T3} is shown in the top panel of Figure 3.7. From this time series, S_{T3} and $S_{<T6,T7,T8>}$ are shown to respond to changes in S in similarly. Further inspection of this figure reveals a offset in the mean value between

S_{T3} and $S_{<T6,T7,T8>}$. This offset in S is a consequence of an offset in the temperature of T3 and $< T6, T7, T8 >$.

The bottom left panel of Figure 3.7 is a scatter plot of S_{T3} against $S_{<T6,T7,T8>}$. Further supporting the time series shown in the top panel, the fluctuations of S_{T3} are clearly similar to the fluctuations of $S_{<T6,T7,T8>}$, with the trend of data points similar to the one-to-one line. An offset is noticeable with the data points typically displaced off of the one-to-one line, towards $S_{<T6,T7,T8>}$. The bottom right panel shows the distribution of the difference between S_{T3} and $S_{<T6,T7,T8>}$. The offset of the temperature measurements is noticeable from the distribution but very small, with the mean of S_{T3} - $S_{<T6,T7,T8>}$ = -0.004. The distribution has a range of ≈ 0.015, which is smaller than the range of S shown in Figure 3.5 (≈ 0.1).

With this data set and using the setup shown in Figure 2.1, it is clear that the displacement of the RTD from the LI-COR has an impact on the calculation of S. The values of S_{T3} and $S_{<T6,T7,T8>}$ is slightly offset as a consequence of the offset in temperature. Some amount of variability is due to the displacement of the temperature sensor in Section 3.1, this is still not enough to account for the wide range of values shown in Figure 3.5.

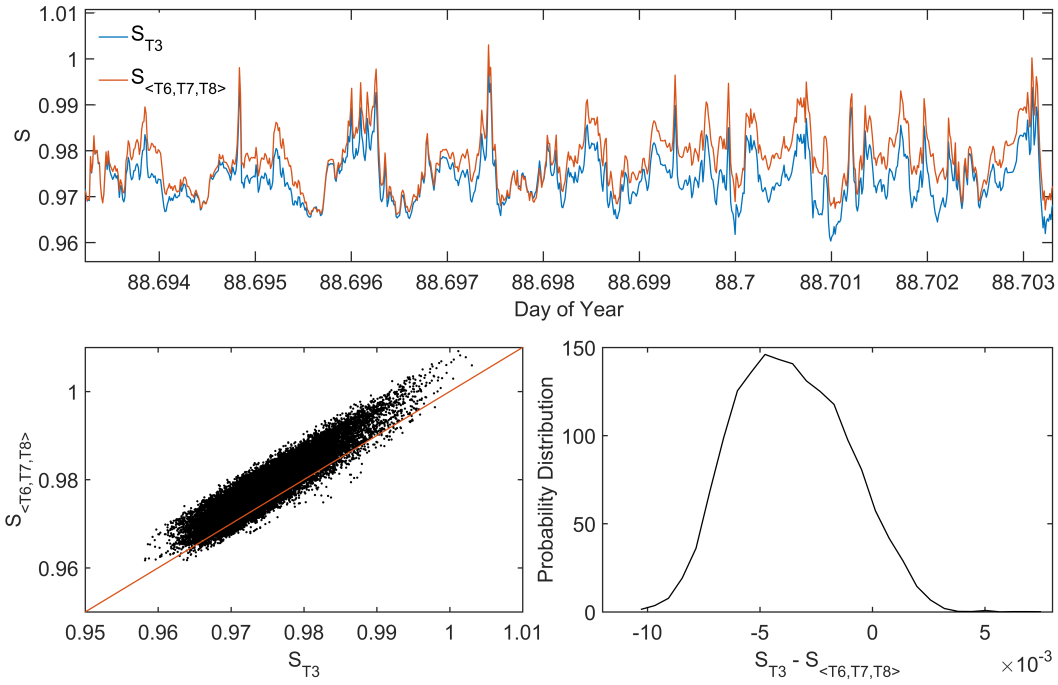

Figure 3.7: Top panel: The time series of the saturation ratio calculated with T3 (S_{T3}) and the saturation ratio calculated with the mean temperature of T6, T7 and T8 at each time step ($S_{<T6,T7,T8>}$); represented as the blue and red lines respectively. Data was taken under moist convection with a temperature difference of 6K between the top and bottom plates of the chamber. In both cases n was converted to 1 Hz. **Bottom left panel:** The scatter plot of S_{T3} against $S_{<}T6, T7, T8>$. The red line is the one-to-one line. **Bottom right panel:** The probability distribution of the difference between S_{T3} and $S_{<T6,T7,T8>}$.

3.3 Cloudy convection

At this point cloud formation is possible as we are in a state of supersaturation; as evidenced in Figure 3.4 and Figure 3.5. However, a cloud is absent due to the lack of cloud condensation nuclei (CCN). In order to better apply these findings to

the atmosphere, we now consider these fluctuations during the formation and in the presence of a cloud.

Figure 3.8 is the time series of water vapor concentration in the chamber for a time before and during the formation of a cloud. At day of year 295.4 $\approx 10^6$ cm^{-3} of NaCl aerosols are injected into the chamber at $\approx 2.5 Lmin^{-1}$. As expected, the mean water vapor concentration immediately decreases as water condenses onto the newly introduced CCN. The decrease in the mean water vapor concentration is 0.06 g m^{-3}.

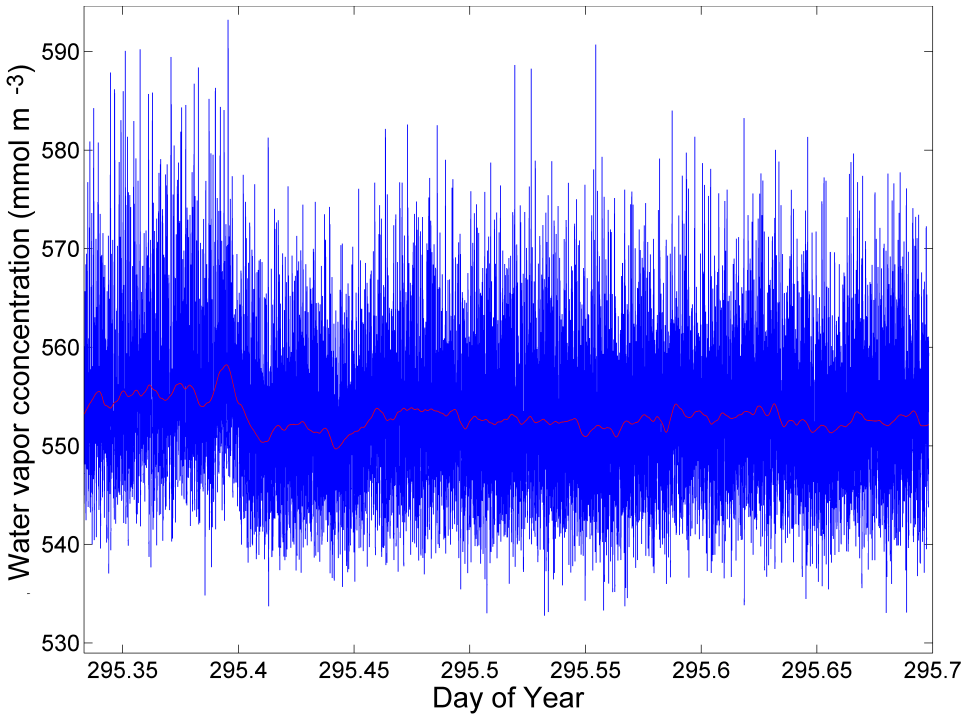

Figure 3.8: Response of water vapor concentration in the chamber (blue line) to cloud formation for $\Delta T = 9$ K. At day of year, 295.4, NaCl aerosol were injected into the chamber, enabling the formation of cloud droplets. Aerosol injection continued for the next seven hours. As the cloud forms, the mean water vapor concentration in the chamber (red line) decreases, as vapor condenses to liquid.

During cloud formation, the variation in n is lowered and as a result S is also lowered. This is consistent with the water droplets acting as a buffer for any turbulent fluctuations. If cloud droplets enter into a region of subsaturation, the droplets will evaporate; raising the local water vapor concentration. Conversely, droplets entering into a region of supersaturation will grow by condensation, lowering the local S so that it is closer to unity. Despite the dampening effect of cloud droplets, there is still significant variability in n, T and S during and after cloud formation.

4. Atmospheric Implications

To this point our focus has been on the fluctuations in the temperature, water vapor concentration and subsequently the saturation ratio. We have shown significant fluctuations about the mean value of S and fluctuations away from the mixing line, calculated from the boundaries of the chamber for moist and cloudy convection. Here we will shift our focus onto the effects these fluctuations have on the atmosphere.

We have already noted that the growth of cloud droplets are affected by the fluctuations in the saturation ratio. The variability we have seen in S, shown in Figure 3.5, implies that there are regions within the volume of an air parcel that have significantly different values for S. There is enough variability for the mean S to be above unity, while regions of the volume are subsaturated; the opposite is also true with the mean S below unity and regions of that volume being supersaturated. For an ensemble

of cloud droplets, this causes some cloud droplets in that volume to be experiencing a higher S than other droplets. This differential in S between neighboring droplets means there is a differential in the growth rate, shown by Equation 1.2, for each droplet in that volume; with some 'lucky' droplets in a higher S growing at a faster rate than the other cloud droplets. As a result of this differential growth rates, the size distribution of droplets in the cloud will broaden, resulting in the enhancement of collision coalescence.

5. Conclusions

Water vapor concentration and temperature were measured in a wet, turbulent environment, which resulted in significant variability in the saturation ratio of water vapor. This variability is prominent during both moist convection with and without the presence of cloud droplets. The variability in the saturation ratio is greater than what would be expected with the water vapor and temperature following the molecular mixing line. It is possible that this is a consequence of the differential diffusivity of water vapor and temperature However, more research needs to be done in order to be certain that this is the case or that some other process is responsible. Regardless, these prominent fluctuations have an effect of broadening the size distribution of cloud droplets due to the difference is growth rates of each droplet. As a consequence, in clouds there is an enhancement of collision coalescence resulting from these fluctuations.

References

[1] Srivastava, R. C. *J. Atmos. Sci.* **1988**, *46*(7), 869–887.

[2] Kulmala, M.; Rannik, Ü.; Zapadinsky, E. L.; Clement, C. F. *J. Aerosol Science* **1997**, *28*(8), 1395–1409.

[3] Shaw, R. A.; Reade, W. C.; Collins, L. R.; Verlinde, J. *J. Atmos. Sci.* **1998**, *55*(11), 1965–1976.

[4] Kostinski, A. B. *Environ. Res. Lett.* **2009**, *4*(1), 015005.

[5] Lamb, D.; Verlinde, J. *Physics and Chemistry of Clouds;* Cambridge University Press: Cambridge, 2011.

[6] Chang, K.; Bench, J.; Brege, M.; Cantrell, W.; Chandrakar, K.; Ciochetto, D.; Mazzoleni, C.; Mazzoleni, L.; Niedermeier, D.; Shaw, R. *Bull. Am. Meteorol. Soc.* **2016**.

[7] Bohren, C.; Albrecht, B. *Atmospheric Thermodynamics;* Oxford University Press: New York, 1998.

[8] Murphy, D. M.; Koop, T. *Q.J.R. Meteorol. Soc.* **2005**, *131*(608), 1539–1565.

[9] Wallace, J.; Hobbs, P. *Atmospheric Science: An Introductory Survey;* Academic Press: San Diego, 1977.